

ISES EuroSun 2016

Annual Performance of a Solar Active House Prototype – Comparing Measurement and Simulation

Jan Steinweg¹ and Gunter Rockendorf¹

¹ Institut für Solarenergieforschung Hameln, Am Ohrberg 1, 31860 Emmerthal

Abstract

A new concept for solar active houses is being tested under practical conditions. While conventional solar house concepts combine large collector areas with large storage volumes (up to 10 m³ in a single family house) in order to achieve solar fractions above 50 %, our new concept only needs small storage volumes (1 m³). To substitute the lack of storage capacity, the new system design uses thermally activated concrete elements directly fed by the solar collector. After having been dimensioned and tested by several simulation studies, a prototype building, equipped with the new heating system, has been constructed and extensively monitored.

The first year of operation already revealed the concept's functionality. During a first monitoring period from April 2015 to March 2016 the recorded data exhibit good agreement with the simulations (based on historical weather data) while storage heat losses are identified as too high. Nonetheless, the annual overall end energy demand for domestic hot water and space heating is 8 kWh/m². This contribution analyses the first year of operation, also covering a peak load test.

Keywords: *solar active house, energy storage, thermally activated concrete elements, TABS, ground heat exchanger, heat pump, experimental study, prototype measurement*

1. Introduction

Previous solar active house concepts combine large collector areas (30...40 m²) and storage tanks (up to 10 m³) with wood stoves as auxiliary heater in order to achieve a combination of high solar thermal fraction (> 50 %) and low primary energy consumption. The new concept presented in this work is aiming at the same high energy efficiency at largely reduced buffer storage volume towards common sizes of about 1 m³, thus allowing buffer installations in the utility rooms, which is particularly favorable in case of energetic retrofit of buildings. As a matter of fact, this approach saves expensive building space, and any maintenance is now possible since all system components fit into standard utility rooms.

The resulting lack of storage capacity is substituted by direct solar thermal activation of already existing masses in the building's concrete slabs. This approach of direct solar thermal room heating has already been evaluated in the 1990's by Papillon (1993) and generates significant advantages. Due to the characteristically low operation temperature of thermally activated building slabs (TABS), a high collector efficiency even at low irradiance levels can be achieved, which is important during the winter months.

The backup heat is provided by a heat pump (HP) coupled to a slender ground heat exchanger (GHX) which receives regeneration by solar thermal heat. Moreover, the GHX is used for the prevention of stagnation during the summer months, thus permanently obtaining the collector's energy delivery readiness. The concept is covering an innovative control strategy for temperature optimized solar heat distribution which has been

designed regarding component and system simulations by Glembin (2012, 2013, and 2014) who has theoretically proven the concept's functionality. For practical testing of this concept, a test building has been planned, built and equipped with the system hydraulics developed according to the outcomes of the simulation studies. The present paper reports results of the first measurement period from April 2015 to March 2016 considering function and performance at monthly and annually scales.

2. System concept and prototype building

Fig. 1 displays the designed energy flows of the solar thermal collector, the heat pump and the different sinks for solar and backup heat. In contrast to simple solar thermal systems, the collector supplies heat to three different heat sinks. A new control strategy developed within the project is applied to utilize the heat fluxes with respect to an optimal effect on the system's end energy savings, see Glembin (2014). According to this strategy both TABS and storage tank may experience positive demand signals, for example during the transitional periods of spring and autumn. The controller then determines the appropriate sink for which the collector is able to gain maximum efficiency. In this case, this may be either a sink provided with a higher priority or a lower demand temperature. As a result of this, the collector can be conducted with very low temperatures starting at 20 °C in cases where the TABS are supplied, and even lower temperatures down to 5 °C in cases of GHX regeneration.

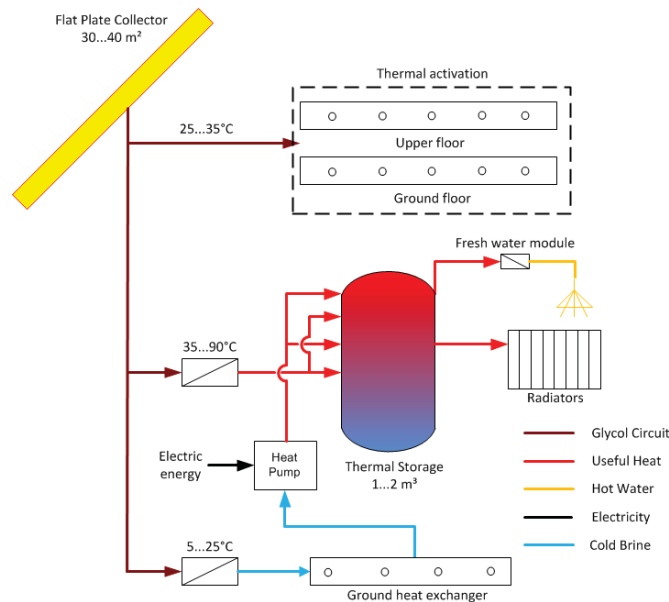


Fig. 1: Scheme of the solar thermal heating system (the lines indicate energy flows)

The test building is located in the urban area of Hanover, Germany, comprising a heated area of 270 m² on three floors; basement (BA) ground (GF) and first floor (FF), and with a nominal annual space heat demand of 39 kWh/m². The building is equipped with a solar collector area of 30 m², facing south with an inclination of 45°. TABS layers, which have been designed for maximum performance with minimum effort using component simulations according to Glembin (2012), are placed in GF and FF. To keep them highly efficient and cost effective, only one distribution loop with central temperature control is used for each floor. The utility room houses a simple buffer storage of 1 m³ from which the domestic hot water preparation (DHW) as well as the space heating demand (SH) are supplied, the latter via conventional radiators. The buffer storage is fed by the solar collector as well as an auxiliary heater, which is a ground coupled compression heat pump. A small horizontal ground heat exchanger with an area of 170 m² serves both as the heat source for the HP and the heat sink for the solar collector's overcapacities during summer. Accordingly, the solar collector can remain in standby for further heat production throughout the summer and experiences almost absent stagnation. Correspondingly, the ground heat exchanger experiences intense regeneration. Therefore, it can be dimensioned significantly smaller than compared to standard design, e.g. due to the German guideline VDI 4640 (2010). A sketch of the concept and a picture of the realized building is displayed in Fig. 2.

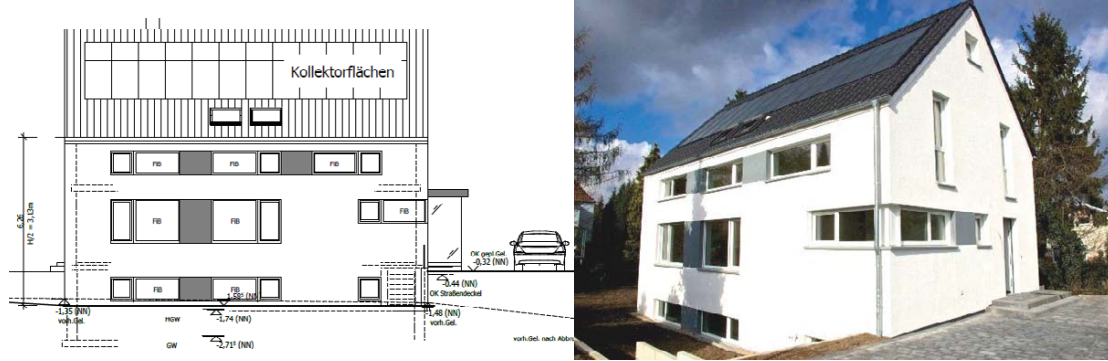


Fig. 2: Sketch of the experimental building during conception (left) and photo of the completed building after the commissioning in January 2015

A central ventilation unit has not been installed so it is up to the inhabitants to set the air change rate by window ventilation. The windows of the GF are equipped with non-automatic external mounted shading elements on the south, east and west façade, as well as the bath and sleeping room windows at the eastern and western façades of the FF. The other windows are (partially) equipped with self-mounted internal shadings. Throughout the phase of measurement, the experimental building has been inhabited by two persons. Further facts of the most important components are given in Tab. 1

Tab. 1: Generic parameters of the main system components of the experimental house

Solar thermal collector	Roof integrated, south, 45° inclination, aperture area 30 m ²
Heat pump (HP)	Brine water compression HP, 8 kW nominal power at 2 kW compressor power
Ground heat exchanger (GHX)	170 m ² area with four distribution circuits (excluding supply pipes), polyethylene pipes with 0.5 m distance
Thermally activated building slabs (TABS)	Approx. 160 m crosslinked polyethylene pipe per slab (ground and upper floor) with 0.5 m distance, bifilar installation, direct connection to glycol circuit of solar collector

3. Measurement and analysis

Measurement concept

The monitoring concept is regarding 65 sensors placed inside and outside the test building and its hydraulic system to gain information about the building's boundary conditions as well as the heating system's performance. The recorded data is evaluated firstly to prove the technical integrity of the concept, including the system controller, the component's interaction and the identification of system and installation issues. Secondly, the system performance will be analyzed by means of indicators such as solar yield Q_{sol} and solar fraction f_{sol} , end energy demand Q_{EE} and the seasonal performance factor SPF of the HP. These quantities are defined by:

$$Q_{sol} = Q_{St} + Q_{TABS,GF} + Q_{TABS,FF} + Q_{GHX} \quad (\text{eq. 1})$$

$$f_{sol} = \frac{Q_{St} + Q_{TABS,GF} + Q_{TABS,FF}}{Q_{St} + Q_{BTA,EG} + Q_{BTA,OG} + Q_{HP,St}} \quad (\text{eq. 2})$$

$$Q_{EE} = W_{el,HP,con} + W_{el,HP,aux} + W_{el,Pump} + W_{el,c} \quad (\text{eq. 3})$$

$$SPF = \frac{Q_{HP,St}}{W_{el,HP,con} + W_{el,HP,aux}} \quad (\text{eq. 4})$$

Q_{sol}	Solar energy gain from collector in kWh
Q_{St}	Solar energy to storage tank in kWh
$Q_{TABS,GF/FF}$	Solar energy to TABS in GF and FF in kWh
Q_{GHX}	Solar energy to GHX in kWh
$Q_{HP,St}$	Energy of HP to storage tank in kWh
$W_{el,HP,con}$	Electrical energy consumption of HP compressor in kWh
$W_{el,HP,aux}$	Electrical energy consumption of HP auxiliary heater in kWh
$W_{el,Pump}$	Electrical energy consumption of the hydraulic pumps in kWh
$W_{el,c}$	Electrical energy consumption of the controller, including energy for all valves in kWh

The system components, the overall hydraulic scheme and the system boundaries regarded by the energy balances are provided in Fig. 3. Technically, the energy flux is balanced through combined mass flux and temperature measurements, calibrated as pairs. The heat sinks (space heating and hot water preparation, blue areas in Fig. 3) are measured by heat meters and the electricity demand of the heat pump, all hydraulic pumps, valves and controllers is measured by electric meters. The thermal comfort of the building is rated through temperature sensors in representative rooms as well as CO₂ and moisture sensors on each floor as indicators for the level of air change due to window ventilation. The data scan interval for all sensors is set to 30 seconds.

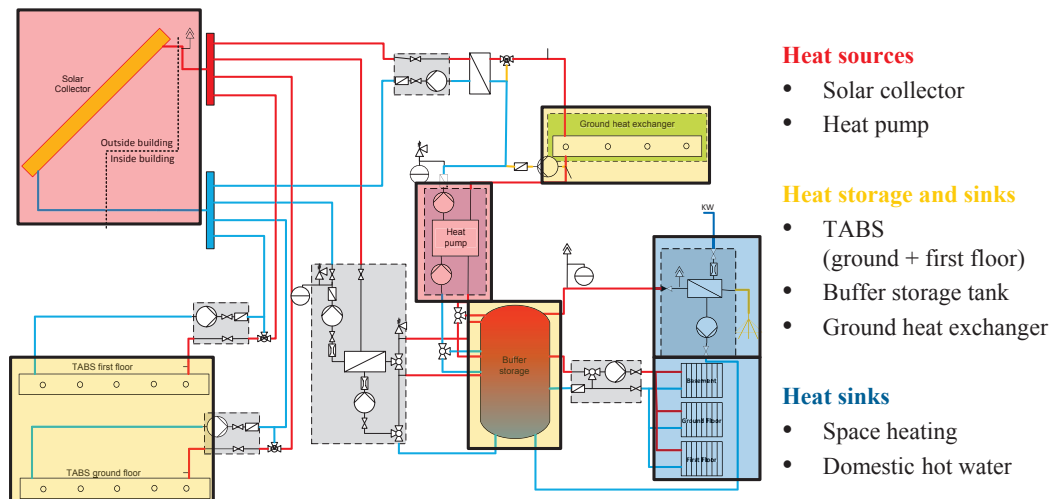


Fig. 3: Scheme of the hydraulic concept of the experimental building including the main components energy balance rooms.

Data analysis concept

We present the system indicators measured during the time period between April 2015 and March 2016 at annual and monthly scales. For further analysis, measurements will be compared to the results of system simulations based on a set of equivalent, historical weather data which had been identified from measurements in the same region during 1989 - 2001. This approach was mandatory for the following reasons:

- Some meteorological data required for the simulation were not measured with the test building, e.g. the ratio of diffuse and direct irradiation, sky temperature, wind speed and ground temperatures.
- Over the course of a year, partially shading of the solar collector and the irradiation sensor occurs, effecting localized signals to sensors and the collector.
- Missing reliable data for the inhabitant's behavior. Room temperatures are not measured building-wide, air change or shading cannot be registered directly at all.

- Some sensor values are considered to be representative for a large area or a component with a wide spread. Examples are again room temperatures but also the core temperatures of the buildings slabs, which are measured with a single sensor and assumed to be equal for the whole room or component.

Hence, to provide consistent simulation parameters, suitable historical weather data are used. As similarity indicators the annual irradiation (on the 45° south inclined surface), the mean ambient temperature and the degree-day numbers are employed and the similarity of the historical and in-situ data are judged by means of least square fit. As result, the best fit was assigned to the weather data of year 1994 which also shows good comparability at monthly scale; hence the 1994 weather data is used as climate environment for the simulations in the sequel. The respective similarity indicators are given in Tab. 2. The remaining differences between the two periods is small indeed, but has to be kept in mind when concluding the results.

Tab. 2: Comparison of the indicator values of the measured year 2015/16 and the historical weather data of Hanover 1994

	Measurement 2015/16	Hanover 1994
Irradiation (45°)	1146 kWh/m ²	1185 kWh/m ²
Degree-day number	3382 Kd	3312 Kd
Mean temperature	10,3 °C	10,7 °C

The useful energy demand, i.e. the energy emitted via the radiators and the domestic hot water, applied to the simulations is adjusted to the measured useful energy of the test building. The simulated space heating energy demand is adapted based on a mean room temperature. To compensate for the situation of partially heating of the building during the monitoring period, the simulations regard a slightly reduced indoor temperature of 19.1 °C. The resulting useful energy demand for space heating (via the radiators) is 5360 kWh/a. The amount of tapped hot water has not been measured. Instead the existing standard domestic hot water demand profile according to IEA Task 44 in Weiss (2003) and Dott (2012) has been adapted to match the respective energy demands of measurement and simulation. Again to adjust to the situation of reduced building usage, the demand profile was scaled by a factor of 0.46 (original data refer to four inhabitants). The resulting energy demand for domestic hot water preparation is 995 kWh.

4. Measurement and simulation results

The following analysis considers measurement and simulation outcomes of the new solar house concept. The comparison is conducted following the method described above. In the first step, annual calculations of the main indicators are compared. In the second part further details are outlined at monthly scale. The following section also concludes the experiences of the peak load tests, which were conducted during February and March 2016.

Annual results

Tab. 3 compares some of the main indicators of both the measured and the simulated building concept which characterize the system performance.

While the overall annual collector yield of ca. 275 kWh/m²a differs slightly only (by 1 %) between measurement and simulation, the spatial supply distribution of the produced solar heat exhibits some differences. The measured energy delivered to TABS contributes by 48 % to the overall solar heat produced, while in the simulation the same share is 64 % (a difference of about 1300 kWh). Analysis of the test building's runtimes shows that TABS are fed by the collector about 25 % shorter than in the simulation. The reasons might be a lower collector performance, larger dead band temperatures or more frequent lock waits due to room temperatures exiting the controller's high limit cut out during the measurement phase.

The lower energy input in TABS in the test building is then compensated by a higher energy input to the storage tank. Consequently, a respective difference of 1300 kWh occurs between measured and simulated storage input, too, such that in sum, the overall energy transfer between TABS and storage input are compensated. The remaining difference of the overall annual data of 1% is leveled by a slightly higher amount

of energy transferred to the GHX while runtimes are almost equal. The stagnation time of the solar collector is 48 h for the simulated system. This only occurs in rare events of GHX outlet temperatures exceeding 25 °C (which is the maximum evaporator inlet temperature of the HP). Since the collector temperature has not been measured, stagnation hours could not be detected directly during the monitoring period.

Tab. 3: Annual results of measurement from April 2015 to March 2016 and simulation based on Hanover weather data of 1994 for the new solar house concept

	Measurement 2015/16	Simulation 1994	Difference
Total solar collector yield	8525 kWh (274 kWh/m ²)	8610 kWh (276 kWh/m ²)	+1 %
To TABS ground floor	1949 kWh (23 %)	2893 kWh (34 %)	+48 %
To TABS first floor	2150 kWh (25 %)	2593 kWh (30 %)	+21 %
To storage	2844 kWh (33 %)	1573 kWh (18 %)	-45 %
To GHX	1295 kWh (15 %)	1094 kWh (13 %)	-16 %
Solar fraction	52 %	54 %	+4 %
Energy HP → Storage	6438 kWh	6006 kWh	-7 %
Total electricity demand	2173 kWh	1875 kWh	-14 %
SPF	3,45	3,69	+7 %

Little deviations exists for the solar gains. The difference between solar fraction of measured and simulated test house is 4%. Slight difference occurs for the energy delivered to the storage by the HP (-7%). Accordingly, the SPF of the HP is 7 % higher in reality than simulated and for the same reason, the total electricity demands differ by 14 %. The difference of the SPF can be explained by the following reasons:

- During October and November 2015, the system controller caused a problem which lead to unnecessary HP running on high temperature level. A major part of that energy got lost via the solar collector to ambient which may explain the 400 kWh higher storage input.
- As of Tab. 2 there are some residual differences in the weather data used for simulation. The mean annual ambient temperatures differ by 0.4 K only, however, between October and March the differences are slightly higher (about 0.7 K). This influences the demand of SH energy and also affects the GHX temperatures.
- The space heating zone inside the storage tank exhibits a mean temperature which is 3.8 K higher during the monitoring 2015/16 as compared to the simulations. This is most likely caused by a lower stratification efficiency of the real storage tank compared to its model. Additionally, the slightly lower ambient temperature mentioned above also has a little impact on the demand supply temperature level of the SH which is calculated with regard to the ambient temperature.

All despite this, the remaining energy demand is very low, especially when considering the sometimes imperfect performance of the system during the first year due to its commissioning. The overall electricity demand (including all electric loads necessary for the annual heat supply) is 2173 kWh or 8 kWh per m² of heated area. Considering primary energy demand, this is passive house level although the measurement period includes commissioning tests and dysfunctions during the first months in 2015 as well as peak load tests during February and March 2016.

Monthly results

To rationalize why a significantly higher share of solar energy is delivered to the storage and how this affects the system performance, Fig. 4 displays diagrams of the monthly solar energy yield distributed to the storage tank and the TABS.

The diagram on the left refers to simulation results which have been concluded in Tab. 3. These are based on a specific parameterization of the storage tank through the design heat loss rate of 5.2 W/K and also taking into account heat losses by thermal bridges and internal recirculation flows according to Wilhelms (2008). The diagram of Fig. 4 (left) shows a pronounced deviation of storage energy inputs between measurement and

simulation during the summer months: here, the measured energy input is 45 % higher between May and August than simulated. Since in this time period the only heat demand results from DHW tapping, which is the same amount at measurement and simulation, the difference must be the consequence of significantly deviating heat losses of the storage tank.

As consequence of this, the test house's storage heat loss rate has been calculated to 7.8 W/K. Some physical reasoning for this could be identified: Considerably circulating flows between the storage tank and its adjacent components (HP and fresh water unit) were located. These flows have been detected with help of the analysis of detailed measurement data and occurred despite the installation of heat traps at the related storage connections. Although further evaluation of thermal bridges supported by thermography did not show any additional indications, other heat loss paths cannot be excluded completely, either. Given by the adverse position of the temperature and mass flow sensors, heat losses of the solar heat transfer unit and the piping are also included in the measured energy delivered to the storage. In consequence to that, the simulation model has been adapted considering these additional heat losses.

The measured overall energy delivered to TABS according to Tab. 3 is almost 1400 kWh lower than in the simulation. As Fig. 4 displays, this difference essentially occurs during the spring and autumn months. This deviation may be rationalized by taking into account passive solar gains and air change rates. The simulated building has an automatic external shading of all east, south and west oriented windows with a threshold total irradiation of 300 W. The air change rate is 0.4 h⁻¹ with an optional night ventilation of 2 h⁻¹ once the room temperature exceed 26 °C. The monitored test building, in contrast, has to be shaded manually and additional, not all of the windows are equipped with effective external shadings. On the other hand, the real air change is low as a consequence of the reduced building usage. As consequence, the simulated passive solar gains are underestimated while the heat losses due to ventilation are overestimated. Though, the TABS threshold room temperature in both cases is 24 °C. If the temperature hysteresis between room and threshold room temperature is lowered by higher solar gains and lower air change the potential for energy delivery by TABS is lowered as well. In sum, this explains the higher active solar energy input to the simulated building.

Taking into account adjusted storage heat losses, improved simulation results are displayed in the right diagram of Fig. 4. We see that the mean deviation between measured and simulated solar energy inputs to the storage tank from May to August has now decreased to 10 %. The measured system performance indicators used in Tab. 3 are again given in Tab. 4 and compared to the new simulation results of the model with matched storage heat losses including the losses of the solar heat transfer station.

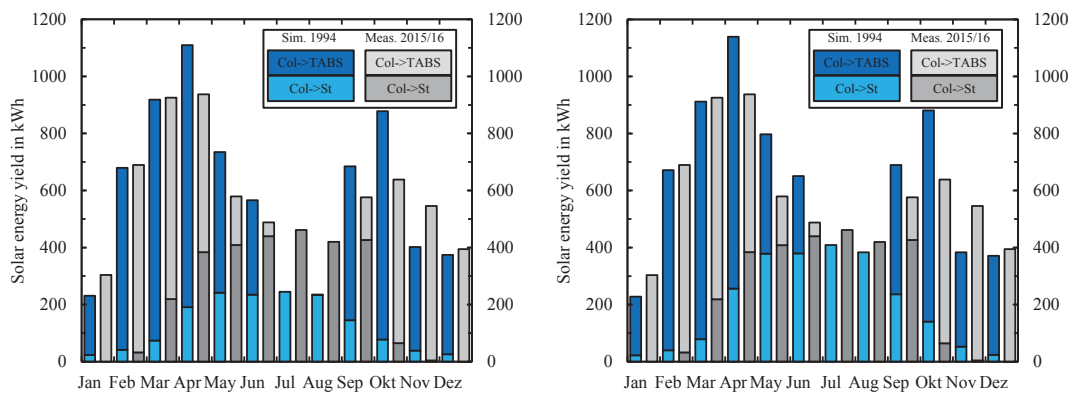


Fig. 4: Comparison of monthly solar energy distribution to storage (St) and TABS for simulation (blue bars) and measurement (grey bars), simulated with design storage heat loss rate (5.2 W/K, left diagram) and heat loss rate of the measured storage (7.8 W/K, right diagram) including heat losses of the solar heat transfer unit

When comparing Tab. 3 and Tab. 4 a slight increase of the solar collector yield is visible. Also the distribution of the solar heat to TABS and storage has changed. The improved results indicate TABS get a 6 % lesser share while the storage supply rises by 9 %. Due to elevated heat losses regarded by the new parameters, the heat transferred to the storage by heat pump also increases by more than 250 kWh. Together with a slight decrease of HP efficiency, the total electricity demand rises by 100 kWh. The solar fraction of eq. 2, in this case it yet

rises to 55 % since the solar yield rises stronger than the heat supplied by HP.

Compared to the measurements, it can be concluded that the difference in solar collector yield increases while the distribution of the solar energy to the different sinks now fits much better. With a solar yield now being a little higher than measured, the performance of the HP, its heat delivered to the storage tank and the total annual electricity demand moves closer to the measured results. Although the shares of the solar heat sinks do not fit perfectly, the order of the heat distribution can be approximated quite well by the simulation. The remaining difference is most likely caused by the different shading and air change parameters.

Tab. 4: Annual results of measurement 2015/16 and simulation (Hanover, 1994) for the new solar house concept with matched storage heat losses

	Measurement 2015/16	Simulation 1994 (matched storage losses)	Difference
Total solar collector yield	8525 kWh (274 kWh/m ²)	8891 kWh (285 kWh/m ²)	+4 %
To TABS ground floor	1949 kWh (23 %)	2610 kWh (29 %)	+34 %
To TABS first floor	2150 kWh (25 %)	2503 kWh (28 %)	+16 %
To storage	2844 kWh (33 %)	2402 kWh (27 %)	-16 %
To GHX	1295 kWh (15 %)	920 kWh (10 %)	-29 %
Solar fraction	52 %	55 %	+6 %
Energy HP → Storage	6438 kWh	6260 kWh	-3 %
Total electricity demand	2173 kWh	1974 kWh	-9 %
SPF	3,45	3,66	+6 %

Peak load tests

From February 23rd to March 29th, the new solar active house system of the test building has been stressed by a peak load test. It was aiming at the evaluation of the remaining thermal backup of the system, especially of the HP and its GHX source as auxiliary heat supply, under practical conditions. A higher load shall be obtained by increasing the room set temperature on the one hand while reducing the available GHX area by 50 % to about 85 m² on the other. This leads to a more frequent HP operation while the heat pump's energy source is significantly smaller.

For the realization of a higher room set temperature the inhabitants have been instructed to adjust the radiator's thermostats by a certain amount. The remaining heating circuit parameters have not been changed, so the threshold room temperature of the TABS remains 24 °C. The resulting mean daily room temperatures of BA, GF and FF during the peak load test are displayed in the right diagram of Fig. 5.

The distribution of the room temperatures remains the same as before the peak load tests. Due to the higher temperature of the utility room situated in the basement, this floor shows the highest temperatures, followed by the GF. As only few rooms of the FF are heated, it has the lowest temperature level. The mean overall temperature ($T_{r,m}$) increases by almost 2.5 K to 22 °C. A related simulation study reveals that this higher room temperature means an increase of the energy demand for SH of 36 %.

The diagram on the right of Fig. 5 displays the soil temperatures ($T_{soil,m}$) measured between the GHX pipes, the daily minimum of the GHX in- and outlet temperatures ($T_{GHX,in,min}$ and $T_{GHX,out,min}$) and the ambient temperature (T_{amb}) during the peak load test. The beginning of the test is clearly remarkable since the daily minimum temperatures of GHX in- and outlet decrease by almost 2 K. Both minimum temperatures remain below zero for the whole test period. While the mean runtime of the HP remains around 20 minutes, the number of cycles of HP operation increases. The reduced GHX area has been achieved by a reduced number of parallel circuits has also been reduced from four to two. This leads to a higher mass flow through the remaining circuits which, in combination with the lower heat exchanger area, also leads to a decrease of fluid temperatures. It is remarkable that the mean soil temperature measured right between the GHX pipes which are arranged with a distance of 0.5 m shows hardly no affection by this temperature decrease. Its temperature runs in closer

accordance to the ambient temperature.

However, the soil temperature at the beginning of the peak load test is almost exactly the same as at the end of the test which most reasonably is caused by the further increasing ambient temperature at the beginning of March. The grey area of the right diagram shows the slowly decreasing amount of energy which is withdrawn from the GHX while the blue area of the left diagram indicates that a significant share of SH energy is already delivered by TABS. In effect, the system withstands the higher thermal loads despite the significantly smaller GHX area very well. Nonetheless, it has to be concluded that the test has been performed quite late in the heating season and with insufficient load demand for a significant stress of the auxiliary heater to its limit. Anyway, the test clarified that the system concept provides considerably heating reserves, which corresponds to recent outcomes of system.

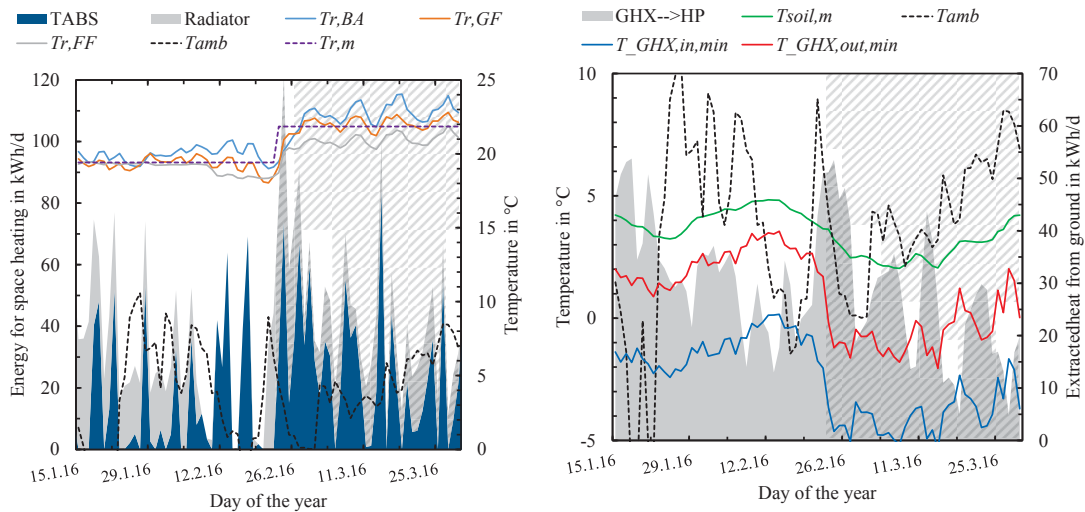


Fig. 5: Room and GHX temperatures during the peak load test, test period in both diagrams marked with hatching
Room temperatures during peak load tests (left): Energy transferred to space heating from TABS and radiators, room temperatures in basement (Tr,BA), ground floor (Tr,GF), first floor (Tr,FF) and mean temperature (Tr,m),
Ground temperatures during peak load tests (right): Energy transferred from GHX to HP (GHX→HP), mean soil temperature ($T_{soil,m}$), ambient temperature (T_{amb}), minimum in- ($T_{GHX,in,min}$) and outlet temperature ($T_{GHX,out,min}$)

Conclusion and outlook

The measurement results of the first year show that the new solar active house concept is already working very satisfying although several initial malfunctions and issues which had to be solved lowered the systems performance. The measured solar fraction of 52 % is already within the expectations. With a remaining overall electricity demand of 8 kWh/m² the primary energy demand is very low. The comparison to system simulations shows a good correspondence but also reveals higher storage heat losses than expected. The losses can mainly be affiliated to unwanted circulating flows through heat pump and fresh water unit. Though heat traps have been provided by the installer as well as a good pipe and component insulation, backflow preventers in the prefabricated components hydraulics were missing almost completely.

The peak load test which has been performed at the end of the heating season was not intensive enough to show the backup heaters limit. Anyway, the current system configuration appears to be well prepared for seasons with higher energy demands. The GHX area might prospectively be further reduced which should be object of further simulation studies.

The missing backflow preventers have now been added, the improvements of controller algorithms, parameters, hydraulics and different performance tests are finished. The GHX temperature has been fully recovered after the end of the peak load test within two months. Since June 2016 a second measurement period is running. The aim is to get results of a full year's period with optimized system performance and no further interference to identify the concepts full potential under practical conditions.

5. Acknowledgement

The project SH-T-Opt Exp (FKZ 032559) is funded by the German Federal Ministry for Economic Affairs and Energy based on a decision of the German Federal Parliament. Project partners of the ISFH are *HELMA Eigenheimbau AG, Lehrte* and *RESOL Elektronische Regelungen GmbH, Hattingen*. The authors are grateful for the financial support. The content of this paper is in the responsibility of the authors.

6. References

Dott, R. et al., The Reference Framework for System Simulations of the IEA SHC Task44/HPP Annex 38, PartB: Buildings and Space Heat Load, a technical report of subtask C, Report C1 Part B, University of Applied Sciences Nordwestschweiz, Muttenz, 2012

Glembin et al., Development of a Concept for the Temperature-Optimized Heat Production in Solar Active Houses, Proceedings of Eurosun Conference, September 18th-20th 2012, Rijeka, Croatia

Glembin et al., Solar Active Building with Directly Heated Concrete Floor Slabs, SHC 2013, International Conference on Solar Heating and Cooling for Buildings and Industry, September 23rd-25th 2013, Freiburg, Germany

Glembin et al., New Control Strategy for Solar Thermal Systems with Several Heat Sinks, Proceedings of Eurosun 2014 Conference, September 16th-19th 2014, Aix-les-Bains, France

Palillon P., Souyri B., Achard G., A new concept for the direct solar floor heating system, proceedings of ISES Solar World Congress, 23.-27. August, Budapest, pp 2328/2234, 1993

Verein Deutscher Ingenieure, VDI 4640 Blatt 1 - Thermische Nutzung des Untergrunds - Grundlagen, Genehmigungen, Umweltaspekte, Beuth Verlag GmbH, 10772 Berlin, Dezember 2011

Weiss, W. (ed.). Solar Heating Systems for houses, a design handbook for solar combisystems, James & James Ltd, London, 2003

Wilhelms, C., et al.: Serienerschaltung von Solarspeichern - eine sinnvolle Systemtechnik?, 18. Symposium OTTI Solar-thermie, Bad Staffelstein, 2008